A High-Pressure Brillouin and Raman Scattering Study on $Na_2FeSi_3O_{8.5}$ Glass: Implications for Pressure-induced Shear Velocity Minima in Silicate Glasses

Anwar Hushur[1,2], Murli H. Manghnani[1], Quentin Williams[3]

[1]University of Hawaii, Hawaii Institute of Geophysics and Planetology, Honolulu, HI 96822, U.S.A.

[2]Xinjiang Key Laboratory of Solid State Physics and Devices, Xinjiang University, Urumqi, China and
School of Physics and Technology, Xinjiang University, Urumqi, China

[3]Department of Earth and Planetary Sciences, University of California Santa Cruz, Santa Cruz, CA 95064 U.S.A. qwilliam@ucsc.edu (Corresponding Author)

Highlights

- High pressure elasticity of a soda-iron silicate glass is investigated to 12 GPa
- Elastic anomalies, including a negative pressure derivative of the shear modulus and an initially nearly pressure-independent Young's modulus, are observed on initial compression.
- Pressure-induced shear velocity minima in silicate glasses are demonstrated to vary systematically with the ratio of network-modifying to network-forming cations.

Abstract

Sound velocities of $Na_2FeSi_3O_{8.5}$ glass have been measured to 12 GPa by Brillouin spectroscopy. Poisson's ratio and bulk, shear, and Young's moduli are calculated as a function of pressure. The shear and Young's moduli and Poisson's ratio show a shift in the response to compression of the glass at ~2.2 GPa, where the pressure dependence of the shear modulus reverses sign. This shift mirrors those of a wide suite of glasses, and further demonstrates that pressure-induced shear velocity minima are general phenomena in silicate glasses containing few network modifiers. Raman spectra have also been collected

of the glass up to 6.5 GPa. A relation is proposed between the magnitude of shear velocity depression observed under pressure in silicate glasses and the ratio of the number of network-modifying cations and network-forming cations. This relation can prospectively be deployed to compositionally tailor the pressure dependence of the elastic velocities of silicate glasses.

1. INTRODUCTION

The elastic constants of silicate glasses under pressure are important for understanding how tetrahedrally-dominated amorphous oxides respond to compaction and differential stress, and are hence a topic of interest within material sciences, condensed matter physics, and the geosciences. For example, the high-pressure behavior of such glasses can be deployed as a constraint on the response to compaction of silicate melts. A range of polymerized silicate glasses have been shown to be elastically anomalous under compression[1-13]. Because of increased resistance to compaction and shear of the structural units, the elastic moduli of most materials increase under pressure. However, a range of silicate glasses have been shown to have elastic moduli (and particularly the shear moduli) that decrease up to pressures of ~ 0.5-3 GPa. For example, both Brillouin and ultrasonic measurements show that the bulk, longitudinal and shear moduli of silica glass soften and exhibit minima near 2 GPa [e.g., 1-4]. This anomalous behavior has been observed using either Brillouin spectroscopy or ultrasonic measurements for a diverse suite of compositions, including water-white glass [5], float glass [6], $MgSiO_3$- and $CaMgSi_2O_6$-glasses [7,10], a range of alumina-bearing glasses [8,10,13], natural basaltic glasses [9,11] and silica-titania glasses [12]. The connection between such anomalous sound velocity trends under pressure and the structures and compositions of glasses has, however, remained unclear. Moreover, whether the presence of abundant iron affects the anomalous pressure dependences of the sound velocities of glasses is not well-constrained.

This study probes the elastic properties of an iron-bearing sodium silicate glass with 95 % enrichment of iron in the ^{57}Fe isotope ($Na_2{}^{57}FeSi_3O_{8.5}$) under high pressure by Brillouin scattering. This particular composition is of interest for a range of reasons. First, it contains trivalent iron almost entirely in tetrahedral coordination [14], and hence it has a ratio of non-bridging oxygens to tetrahedral cations of 0.25. As such, its structure is dominated by network-forming cations, but contains a comparatively small quantity of non-bridging oxygens, as well as network-modifying cations. It is accordingly a model glass for examining systems with limited amounts of depolymerization. Second, it is a transition-metal bearing analogue of sodium aluminosilicate glasses, the properties of which are relevant for both ceramics and earth materials, and it is unclear whether the structural and elastic changes that occur within an iron-bearing silicate glass differ from those in aluminosilicate glasses under compression. Third, the structural and elastic properties of iron-rich glasses are of interest because both naturally-occurring geologic melts and synthetic glasses designed to isolate toxic and radioactive material often have substantial iron contents within them [e.g., 15].

Brillouin scattering, the inelastic scattering of light induced by acoustic phonons, is commonly deployed to determine sound velocity and elastic constants. This optical technique requires no mechanical contact with the sample and allows experiments on samples of order microns in dimensions, and hence is ideally suited to measure sound velocities under extreme conditions in a diamond anvil cell. These velocity data were initially measured to provide density constraints for high-pressure measurements of the vibrational density of states (DOS) of this glass using nuclear inelastic scattering [14], with a particular focus on the origin of the boson peak in this glass, and its similarity at high pressures to the transverse acoustic singularity of the corresponding crystal. However, a quantitative analysis of these elastic data has not been presented. Here, these data are deployed in conjunction with previous elastic results on silicate glasses under pressure to provide structural/compositional systematics for the anomalous low-pressure elastic properties of polymerized silicate glasses. These data also show the capability of the Brillouin scattering technique to determine the elastic constants for semi-transparent samples using the platelet geometry.

2. EXPERIMENTAL DETAILS/METHODOLOGY

The ambient-pressure glass transition temperature of this composition is 723 (±1) K [14], which is close to that of binary sodium silicate glasses [16,17]. It has a density of 2.714 g/cm^3, which is larger than those of binary sodium silicate glass and sodium aluminum silicate glass due to the substitution of iron. Due to the presence of iron, the bulk glass aliquot is opaque. After polishing to 30 μm thickness, it is semi-transparent with a dark yellowish color. Permanent densification has also been observed for this glass at 1, 2, and 3 GPa at a temperature of 673 K, or ~90% of the glass transition temperature in this material [18], with an emphasis on the vibrational density of states of these densified glasses.

The Brillouin scattering experiments were conducted by exciting the sample in a diamond anvil cell (DAC) with 480 μm diameter culets and using the 514.5 nm green line of a Spectra Physics Ar-ion laser (the output beam power is 130 mW, and in front of the DAC, the beam power is 60 mW). The semi-transparent glass sample was 80 × 70 × 30 μm thick and was mounted in a 170-μm diameter hole in a pre-indented stainless steel gasket of 40 μm thickness. Two pieces of ruby ~ 6 μm in size were placed near to the two sides of the sample for pressure calibration. Liquid argon was loaded as a pressure-transmitting medium using a standard liquid nitrogen-based loading technique. The pressure was measured using the shift in the R1 line of the rubies loaded along with the sample. Spectra were recorded in the 70º platelet-scattering geometry with no polarization used for the collected signal. In order to obtain the refractive index, Brillouin measurements were also performed in the backscattering geometry at ambient pressure.

Since Doppler-shifted light photons scattered from thermally excited acoustic phonons (sound waves) of the sample produce peaks in the Brillouin spectrum, the sound velocity (V) is expressed as:

$$V = \frac{\lambda \nu}{2n \sin(\theta/2)} \quad (1)$$

where v is the Brillouin frequency shift, λ is the wavelength of the laser, n is the refractive index of the sample, and θ is the scattering angle. We deploy both the back-scattering (θ = 180°) and platelet geometries. Whereas the classical backscattering geometry enables only measurements of nV_P (the product of refractive index and longitudinal velocity), the platelet geometry (Figure 1) allows us to measure the sound velocities (V_P and V_S) directly and independently without knowledge of the refractive index according to the relation,

$$V = \frac{\lambda \nu}{2 \sin \Theta} \quad (2)$$

where Θ is the angle between the incident light and the normal to the surface of the sample. In this study, the angle is typically chosen as 35°.

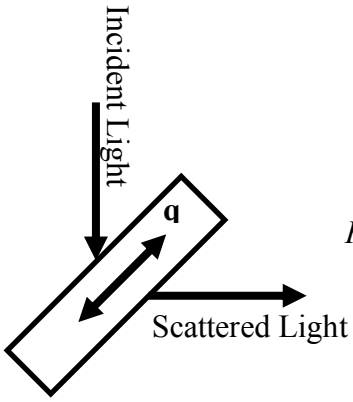

Figure 1. Platelet geometry for Brillouin scattering.

The two scattering geometries also provide the ability to determine the refractive index n of the glasses directly. Since the velocity of an acoustic phonon in an anisotropic medium is independent of direction, the ratio of the Brillouin shifts, as expressed as the Brillouin shifts in the platelet geometry divided by the Brillouin shifts in the back scattering geometry, is equal to $n/\sin\Theta$. By taking the ratio of the Brillouin shifts at different pressure points, the refractive index n of the glass can be uniquely determined both at ambient conditions, and as a function of pressure. At ambient pressure, the index of refraction of this glass is determined to be 1.627 (±0.001), which is comparable to those of other transition metal-bearing sodium silicate glasses [19].

Raman spectra were collected both at ambient and high pressures, and following quenching from high pressures, of this glass. The Raman spectra were recorded using a triple pass Dilor XY spectrometer equipped with a liquid nitrogen-cooled charge-coupled-device

(CCD) detector. The 514.5 nm green line of an Ar ion laser was used to excite the sample. The laser light was focused with a Mitutoyo long distance 50× objective to a spot of about 2 μm diameter in the sample with the laser power being 30 mW on the sample. The spectrometer was calibrated using single-crystal silicon as a reference.

For the high-pressure Raman measurements in the diamond anvil cell, a finely polished glass fragment 50 × 40 × 20 μm in size was mounted in a rhenium gasket in a diamond-anvil cell equipped with 350 μm diameter culets. Two pieces of ruby ~5 μm in size were placed on the two sides of the sample for pressure calibration. As with the Brillouin measurements, liquid argon was loaded as a pressure-transmitting medium, and pressures were estimated using the shift in the R1 line of the rubies loaded along with the sample. All spectra were recorded using an unpolarized backscattering geometry.

The density of the glass at high pressures is obtained using the velocity data in Table I from:

$$\rho_P - \rho_o = \int_{P_o}^{P} \frac{\gamma}{V_B^2} dP \qquad (3)$$

Here, ρ_p and ρ_o are the density of $Na_2FeSi_3O_{8.5}$ glass at pressure P and ambient pressure P_o, respectively, and V_B is the bulk sound velocity of the glass. γ is the ratio of the specific heat at constant volume and pressure (C_P/C_V, which we presume to be 1, in accord with Richet and Bottinga [20], who have shown this parameter to be within 0.2% of unity at 300 K for alkali silicate glasses). This latter parameter is present to convert the isentropic velocity/moduli determined in the Brillouin experiment to isothermal conditions. For elastically isotropic materials,

$$V_B^2 = V_P^2 - 4V_S^2/3 \qquad (4)$$

where V_P and V_S are the longitudinal and transverse sound velocities. The calculated densities as a function of pressure are used to extract the high pressure elastic moduli from the velocity data using $\mu_p = \rho_p V_S^2$ and $K_p = \rho_p V_B^2$, where μ_p is the shear modulus at pressure and K_p is the bulk modulus at pressure.

3. RESULTS AND DISCUSSION

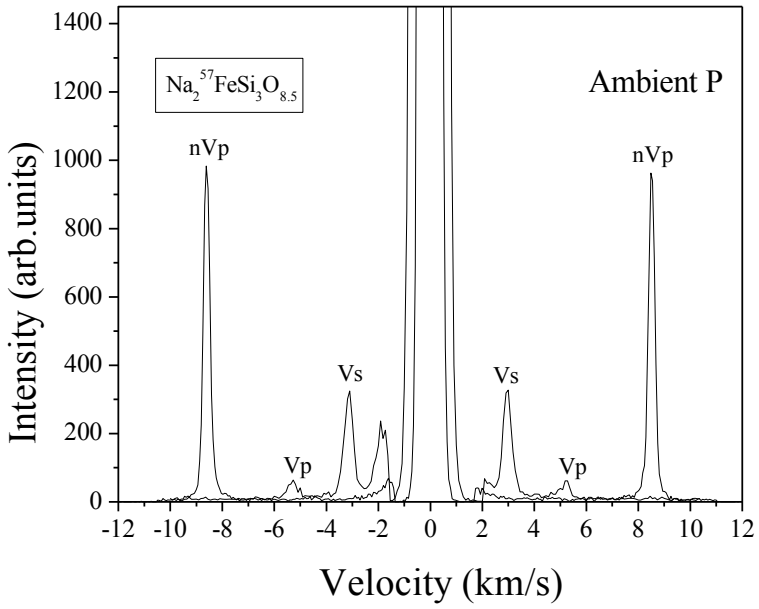

Figure 2. Brillouin spectrum of $Na_2{}^{57}FeSi_3O_{8.5}$ glass at ambient pressure measured in both platelet geometry and backscattering geometry (the spectrum labeled with nV_p).

Figure 2 shows representative Brillouin spectra at ambient pressure in both platelet and backscattering geometry: clearly, the amplitude and character of the peaks is sufficient to accurately determine the three parameters of interest: the compressional and shear velocity, and the index of refraction. Importantly, as the peak locations are symmetric across the incident laser line (corresponding to both Stokes and anti-Stokes scattered light), there is redundancy in determining the location of relatively weak peaks, such as the V_p-associated band.

High pressure Brillouin spectra are shown in Figure 3 in the platelet geometry, with the resultant velocities at ambient and high pressure given in Table I. Our ambient pressure velocity determinations agree well with a previous determination [18] Figure 3 shows that the Brillouin peaks associated with both the shear and compressional peaks are well-resolved: the peak from the argon pressure medium crosses over the shear peak near 3 GPa, but it otherwise does not affect the measurement of the sound velocities in the glass. Figure 4 shows the shifts in compressional and shear velocities with pressure. The shear velocity initially decreases with pressure up to a minimum value at ~2.2 GPa; at higher pressures, it has a positive pressure dependence. Correspondingly, the compressional wave velocity

has a small but positive initial pressure shift, which markedly increases above ~2.2 GPa. Such anomalous negative (or small, for V_P) shifts are relatively commonly observed within silicate glasses on initial compression [1-13]. The depression in shear velocity in this iron silicate glass is quite close to that observed within a float glass measured using the same techniques and apparatus under compression [6], indicating that two glasses with markedly different compositions, and differing degrees of polymerization, have similar shear velocity behavior under compression.

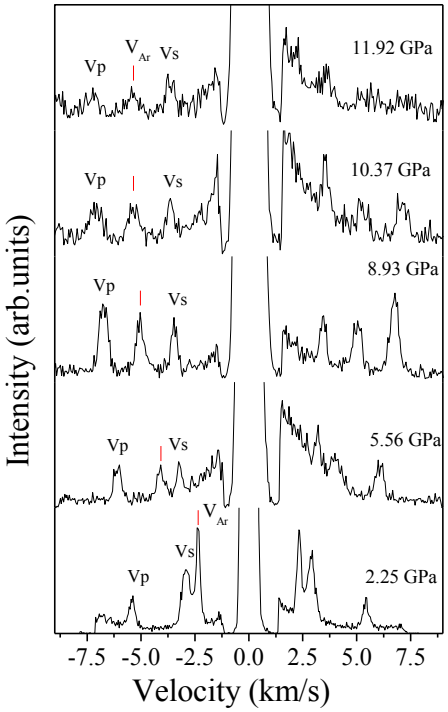

Figure 3. Brillouin spectra of $Na_2FeSi_3O_{8.5}$ glass at various pressures measured in platelet geometry. Red markers denote peaks from Brillouin scattering of the argon pressure medium.

TABLE I. Sound velocities of $Na_2FeSi_3O_{8.5}$ glass at high pressure determined by Brillouin scattering (upper values are from the first run, lower values from the second run). Errors are given in parentheses.

Pressure (GPa)	*Vp* (km/s)	*Vs* (km/s)
1.00E-04	5.261 (16)	3.050 (2)
2.25	5.41 (2)	2.930 (8)
4.04	5.801 (8)	3.11 (1)
5.56	6.07 (1)	3.207 (10)
7.11	6.30 (1)	3.32 (3)
8.93	6.745 (9)	3.45 (1)
10.37	6.96 (2)	3.55 (1)
11.92	7.18 (6)	3.65 (3)
1.16	5.28 (3)	3.012 (9)
1.7	5.34 (2)	2.967 (7)
2.3	5.410 (9)	2.926 (4)
3.2	5.68 (1)	3.013 (7)
4.2	5.92 (2)	3.08 (3)
5.2	5.99 (3)	3.23 (2)
6.8	6.36 (3)	3.32 (2)

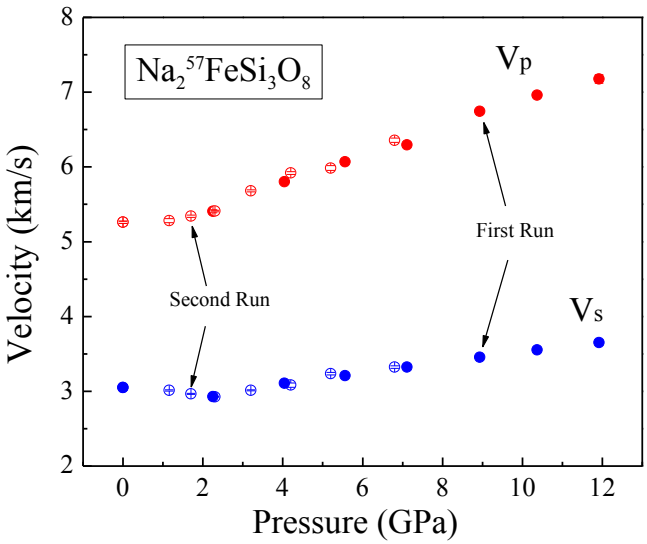

Figure 4. Sound velocity of $Na_2FeSi_3O_{8.5}$ glass at various pressures determined by Brillouin scattering (First and second run). Errors are smaller than the symbols, and are illustrated for the second run (open symbols).

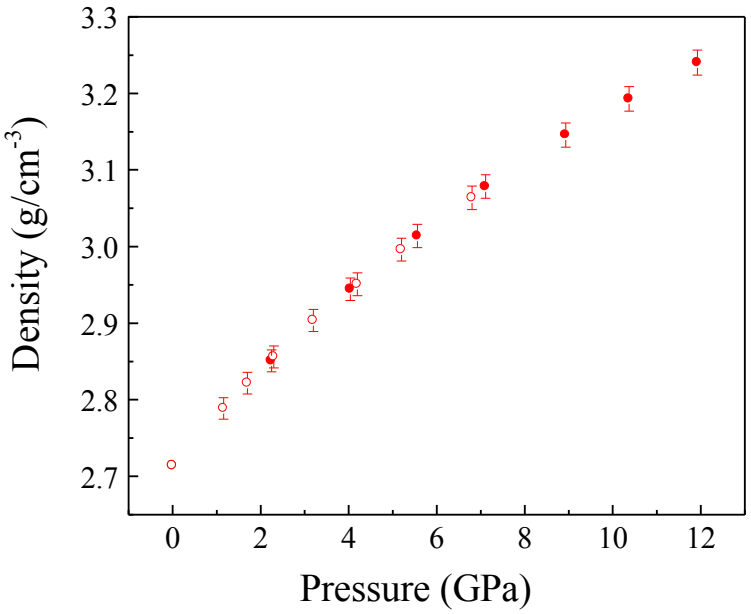

Figure 5. Density of $Na_2FeSi_3O_{8.5}$ glass at various pressures determined by Brillouin scattering in conjunction with Eqn. 3 (solid and open symbols are first and second run, respectively).

Figure 5 shows the calculated densities of this silicate glass under compression: the magnitude of elastic and irreversible densification (~17%) is somewhat less than that of end-member silica (~23%) [e.g., 2] over the pressure range to 12 GPa, reflecting the slightly higher bulk modulus of this glass relative to pure silica. Figure 6 shows the variation in bulk modulus and shear modulus with pressure. As indicated by the trend in the compressional wave velocity, the bulk modulus appears to initially shift shallowly (Figure 6a), with the trend above ~1.5 GPa being monotonic and nearly linear. Within this higher pressure interval, the derivative of the bulk modulus (dK/dP) with respect to pressure is slightly in excess of 6: this linearity, and comparatively normal value of dK/dP, indicates that pervasive coordination changes of the silicon cations are unlikely to initiate in this material up to our peak pressure of 12 GPa. The onset, and progressive occurrence, of such coordination changes in glasses has been associated with a markedly enhanced pressure derivative of the bulk modulus [7]. Figure 6b shows that a pronounced minimum in the shear modulus occurs near 2.25 GPa, with higher pressure results again showing a nearly linear increase with compression.

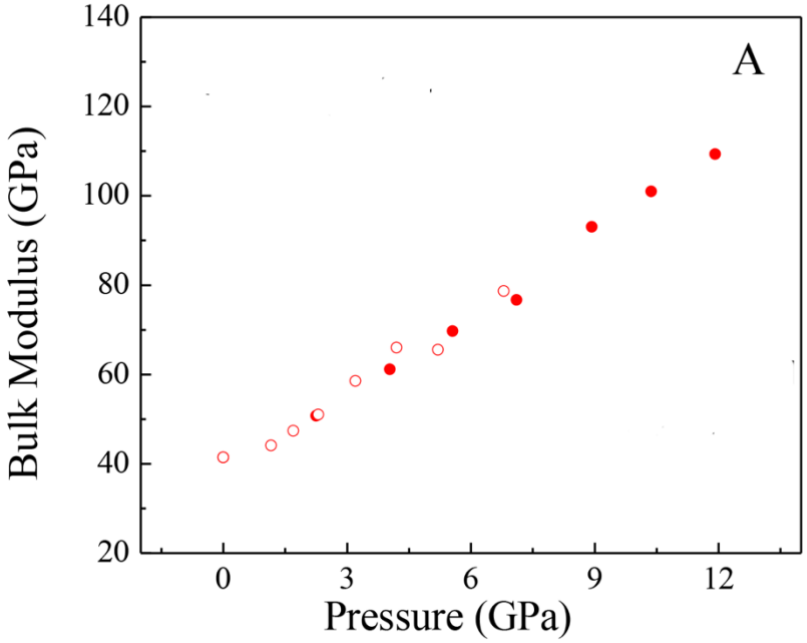

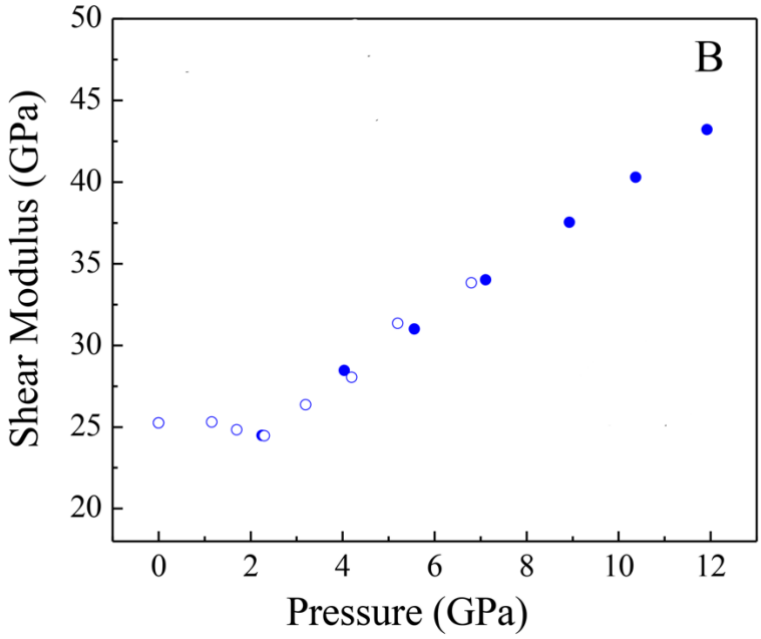

Figure 6. (A) Bulk moduli of $Na_2FeSi_3O_{8.5}$ glass at various pressures determined by Brillouin scattering (First and second run). (B) Shear moduli of $Na_2FeSi_3O_{8.5}$ glass at various pressures determined by Brillouin scattering (first and second run are solid and open symbols, respectively). Error bars are comparable to, or smaller than, the size of the symbols.

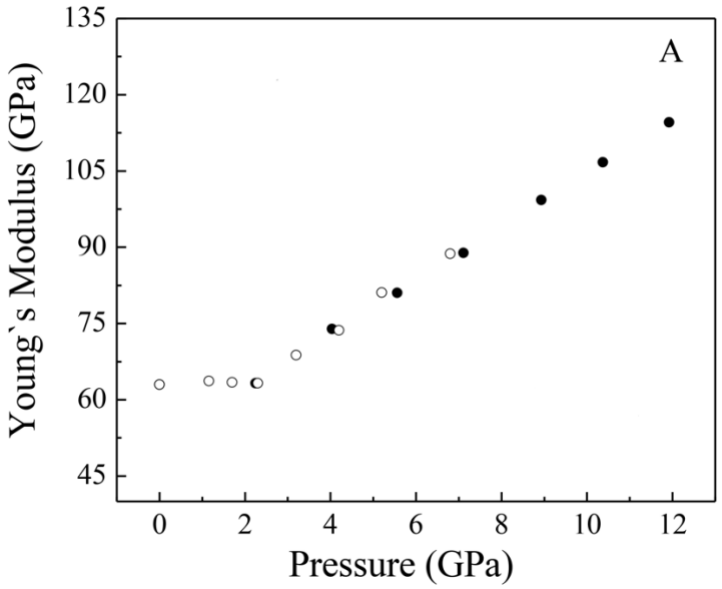

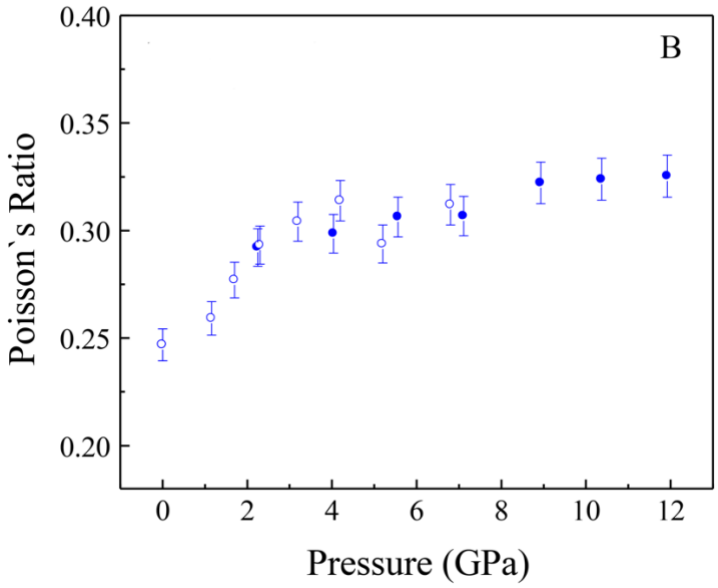

Figure 7. (A) Young's moduli of $Na_2FeSi_3O_{8.5}$ glass at various pressures determined by Brillouin scattering. Error bars are smaller than, or comparable to, the size of the symbols. (B) Poisson's ratio of $Na_2FeSi_3O_{8.5}$ glass at high pressures determined by Brillouin scattering (closed and open symbols are for the first and second run).

This anomalous behavior of the shear modulus is directly reflected in the Young's modulus and Poisson's ratio of this glass (Figure 7a, b). Young's modulus is nearly constant up to 2.25 GPa (Figure 7a), while Poisson's ratio increases markedly from ~0.25 to ~0.3 in this pressure range before modestly increasing to the highest pressures of these measurements. Poisson's ratio is of particular interest, as a general inverse correlation has been drawn between its value and the 'free volume' fraction in glasses, as manifested by the atomic packing density [21]. Thus, there is a possible conceptual relationship between the negative pressure dependence of the shear modulus, the associated comparatively large initial pressure shift of Poisson's ratio, and an anomalous shift in packing of the glass on its initial compression.

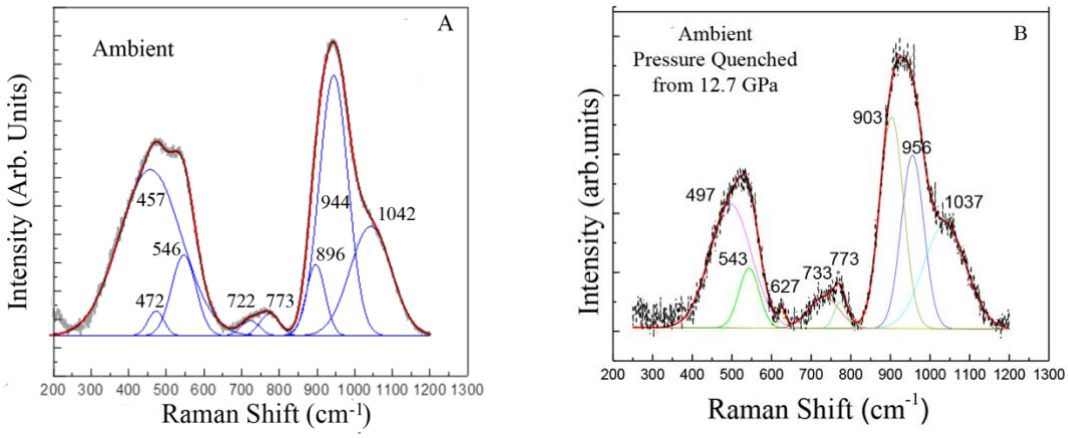

Figure 8. (A) Raman spectrum of $Na_2FeSi_3O_{8.5}$ glass at ambient pressure, prior to compression. (B) Raman spectrum of the pressure-quenched sample from the higher pressure Brillouin experiment.

The degree to which the observed changes in elastic properties reflect the elastic characteristics of the ambient glass, as opposed to irreversible densification, may be assessed from complementary Raman data on this glass. Figures 8a and 8b show Raman spectra of the glass before compression, and after compression to 12.7 GPa. Based on the differing polarization of bands, Wang et al. [22] attributed the bands at 457 and 944 cm^{-1} to the symmetric stretch of oxygens bridging between fully polymerized tetrahedra, and the asymmetric stretch of those oxygens, respectively. The shoulders at 549 and 1067 cm^{-1} are assigned to vibrations of bridging oxygens and non-bridging oxygens associated with Q^3 species (tetrahedra with three bridging and one non-bridging oxygen). Among the higher frequency peaks, there has also been a component of an FeO_4 tetrahedral stretching vibration proposed to be present [e.g., 23]. Following compression to 12.7 GPa, the peak initially at 457 cm^{-1} has migrated irreversibly to higher frequency: a result compatible with narrowed T-O-T angles in the decompressed glass [22]. *In situ* Raman spectroscopy of the

glass at high pressures (Figure 9) demonstrate that these irreversible changes in morphology of the low frequency peaks do not occur up to at least 6.5 GPa, and hence their onset must lie between 6.5 and 12.7 GPa. Therefore, our observations of the velocity minimum in this material are associated with purely elastic behavior of the glass, and are not expected to be affected by irreversible compaction. Importantly, this loose constraint on the onset of irreversible behavior is compatible with the onset of irreversible compaction in silica glass, which occurs near 8.6 GPa at 300 K [24].

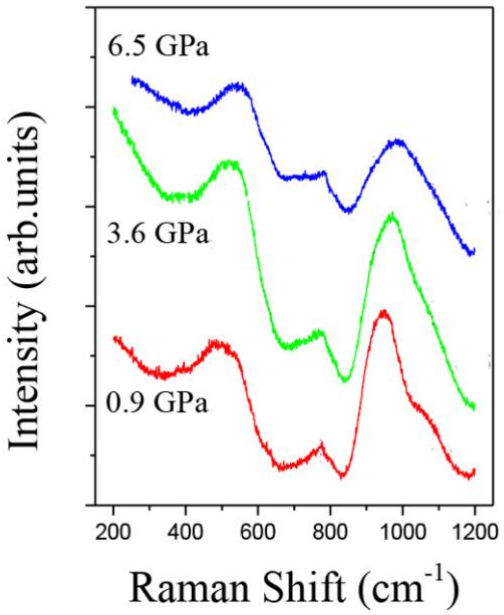

Figure 9. In situ Raman spectra of $Na_2FeSi_3O_{8.5}$ glass at high pressures.

A key question emerges from the elastic data: what structural or chemical effects may produce the size of the minima in shear velocity and modulus shown in Figures 4 and 6b, and which are reflected in the dramatic increase in Poisson's ratio in Figure 7b? Such minima are well-known within silicate glasses under pressure and, as in this study, are more often observed in shear velocities than in compressional velocities [2,3,5-7,9,14]. Indeed, the magnitude of the shear velocity depression directly reflects the anomalous elasticity of these glasses. Perhaps the most diagnostic experiments to date on the origin of these anomalies have involved the observation that these minima are suppressed in silica glass in a helium medium [25-27]. The mechanism for this suppression has been attributed to He entering into large sites/voids within the structure, and preventing their pressure-induced collapse [25,27]. Our interpretation of these results (which involve incorporation of He at the 1 He per Si atom level or greater) modestly differs: He is well-known to enter large cavities asymmetrically, being attracted to cations [28]. And, the prospective role of He in restricting the Si-O-Si bond angle from bending has long been appreciated from modeling [29]. Therefore, our interpretation of the elastic minima involves non-networking

forming atoms (or ions) within the structure playing a pivotal role in restricting the flexibility of Si-O-Si(Al) angles in silicate glasses, and hence narrowing the broad Si-O-Si potential minimum that produces the initial large degree of flexibility of the network (and hence the velocity softening). Subsidiary support for the interpretation that the flexibility of tetrahedral networks is critical in generating these elastic anomalies is derived from the observed negative shear velocity gradients observed in non-silica-containing calcium aluminate glasses [30]: the general phenomenon of anomalous elasticity hence hinges on the presence of a tetrahedral framework, rather than being solely confined to silica-dominated networks.

The absence of, or reduced amplitude of, a pressure-induced velocity minimum has been correlated with greater degrees of compositionally-induced depolymerization of silicate glasses [8,10,11]. However, the observation that the current $Na_2FeSi_3O_{8.5}$ composition glass has a maximum shear velocity depression under pressure similar to that of a less polymerized float glass [6] raises the possibility that depolymerization may not be the sole feature that drives these velocity depressions. Indeed, these silicate glasses have NBO/T ratios of 0.25 and 0.7, respectively, and their maximum depressions in shear velocity are -4.1 and -5.1% (which is the opposite trend from that expected from the depolymerization-smaller velocity minima trend). However, the ratio of their number of network-modifying cations to their network-forming cations is essentially identical. Accordingly, we hypothesize that the introduction of network-modifying cations into the glass reduces the flexibility of a subset of the polymerized linkages in the glass. In this regard, it is critical to note that atoms/ions need not lie within the apex of the Si-O-Si(Al) bond angles whose flexibility they impact: even atoms that neighbor the tetrahedra on the O_3 side of the O_3Si-O-SiO_3 linkage (or, juxtaposed with non-bridging oxygens) dramatically impact the width of the Si-O-Si potential minimum [29].

Figure 10 shows the maximum percentage change in shear velocity depression under pressure within a broad range of non-densified silicate glasses. Clearly, relatively modest amounts of network-forming cations dramatically decrease the amount of maximum shear velocity depression, but a modest velocity anomaly persists even when relatively large amounts of network modifiers are incorporated into the glass. Notably, our interpretation of the structural effect that suppresses the elastic minima differs subtly but significantly from past interpretations: rather than viewing the suppression as an effect of depolymerization, we propose that the suppression is a consequence of interactions between network-modifying cations and the polymerized structures within the glasses. Our analysis implicitly treats the principal effect of network-modifying cations as occupying free volume within the glasses, and hence restricting the deformability of the surrounding polymerized framework. The role of free volume (and its availability/occupancy) is supported by the observation that pressure-densified silica glasses, and particularly those densified at simultaneous high-pressure and -temperature conditions, also have the anomalous elastic effect suppressed [31,32]. A complementary view of the trend in Figure 10 is that it reflects a continuum between polymerized systems, with ‘floppy’ connections between comparatively rigid silica tetrahedra [33], to systems that involve higher average coordination numbers. The higher degrees of connectivity associated with more network-modifying cations [e.g., 34, 35] may lead to progressively less anomalous rigidities as more highly-coordinated cations are incorporated into the glass. This continuum is likely also relevant to tendencies in thermal expansions as well: silicate glasses with larger proportions

406 of network-modifying cations have larger thermal expansions than the low thermal
407 expansion associated with fully polymerized silica, or silica-titania, glasses [36-39]. This
408 interpretation of velocity depression as being induced by a trade-off between connectivity
409 and floppy connections may also illuminate the role of irreversible densification of glasses
410 in eliminating these velocity minima within glasses with notably different degrees of
411 polymerization [2,4,7,8]. For densified glasses, it is possible that 'floppy' connections are
412 suppressed by the narrowed T-O-T angles within the irreversibly densified glasses. In this
413 perspective, irreversible densification may alter not only the bond angles between rigid
414 polymerized units, but also the interactions between the network-modifying cations and
415 the rigid units. Indeed, a shift in the structural role of network-modifying cations in the
416 pressure range in which irreversible densification occurs has been observed in $MgSiO_3$ and
417 $CaSiO_3$ glasses [40].

418 One notable aspect of Figure 10 is that it incorporates data on a wide suite of compositions
419 of glasses (spanning from natural alkaline earth-dominated aluminous silicate
420 compositions to multi-component synthetic alkali-rich compositions with silica as the sole
421 network former), and a number of separate high-pressure investigations with variable
422 densities of data sampling (for which coarser data sampling would cause a potential
423 underestimate in the maximum value of velocity depression). As such, despite the broad
424 range of compositions and studies, a gross trend of decreasing velocity anomaly with the
425 relative amount of non-network forming cations is observed. Clearly, the identity of
426 substituted cations also play a role in the magnitude of velocity depression: large alkali
427 cations (such as K) clearly induce smaller velocity depressions than divalent cations [13];
428 yet, this effect appears to be smaller than the normalized number of network modifiers
429 present within the glass. Thus, Figure 10 provides guidelines for, when advantageous,
430 tuning the composition of glasses to produce differing degrees of pressure-induced shear-
431 velocity depression. As an aside, although all the glasses in Figure 10 show decreased
432 compressional velocity slopes at low pressure, only silica, obsidian, and the two chemically
433 complex basalts show clearly negative initial V_p slopes, implying that either complex
434 natural compositions and/or the presence of Al is critical in producing negative shifts in
435 the compressional velocity.

436

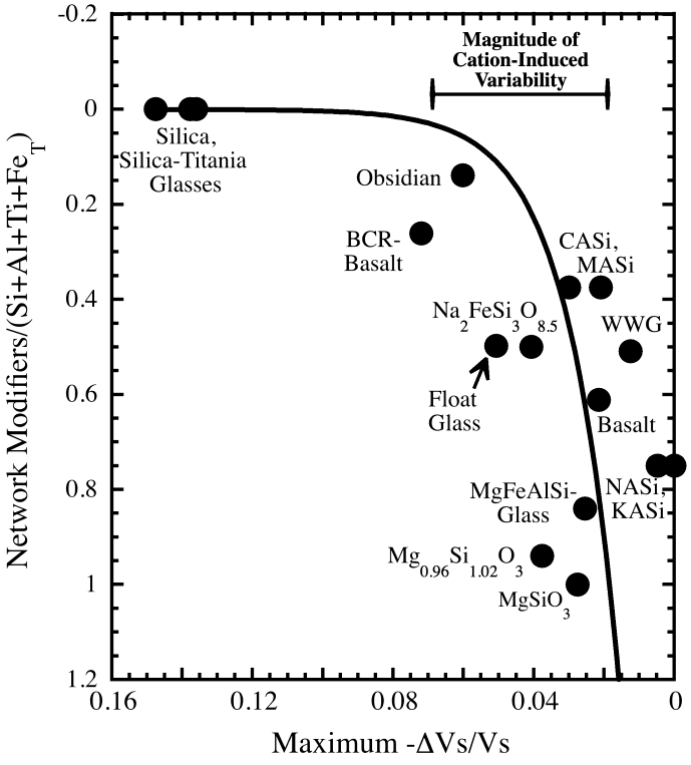

Figure 10. Dependence of the maximum amount of shear velocity depression (normalized to the ambient pressure shear velocity) observed in a range of silicate glasses under compression on the number of network modifying cations (Mg, Ca, Na, K) relative to network formers (Si, Al, Fe^{3+}) within the glass. Data for silica [2], silica-titania glasses [12] (2 compositions), obsidian [3], water-white glass (WWG) [5], a float glass [6], basalt [9], $MgSiO_3$ [9], and $Mg_{0.79}Fe_{0.1}Al_{0.1}Si_{0.96}O_3$ [9] compositions, an oxidized Columbia River (BCR) basalt [11], a $Mg_{0.96}Si_{1.02}O_3$ composition [7], $Mg_3Al_2Si_6O_{18}$, $Ca_3Al_2Si_6O_{18}$, $Na_3AlSi_3O_9$, $K_3AlSi_3O_9$ compositions [13] (MASi, CASi, NASi and KASi) and $Na_2FeSi_3O_{8.5}$ composition (this study) are shown. The results of [10] are excluded because they did not measure ambient pressure velocities of their samples, with their measurements initiating between 0.8 and 1.4 GPa. Where present, the oxidized Fe_2O_3 component is treated as a network former in all cases. The line is an exponential fit to the data and is intended to guide the eye. The first-order trend is associated with the network-modifier/network-former ratio, while the horizontal variability in the plot appears to be associated with the effect of different cations on the depression of the shear velocity [13]: the zero-velocity depression of $K_3AlSi_3O_9$ (KAS) relative to the depressions of the Mg-silicate glasses illustrates this effect. The range at the top illustrates the approximate magnitude of this cation-induced effect.

4. CONCLUSIONS

The elastic properties of $Na_2FeSi_3O_{8.5}$ glass have been measured to pressures of 12 GPa using Brillouin spectroscopy: our ambient pressure results incorporate both measurements in platelet and backscattered geometry, while our high-pressure results deploy the platelet geometry. The results demonstrate that there is a substantial decrease in shear velocity and modulus that reaches a minimum at ~2.2 GPa. The corresponding compressional velocity and bulk modulus (as well as the Young's modulus) show anomalously low positive increases up to this pressure. Hence, abundant trivalent iron (as a network former) within this glass does not appear to markedly affect the anomalous elastic behavior of silicate glasses under compression. The systematics of the elasticity of a wide range of silicate glasses under pressure indicate that such anomalous decreases in the shear velocity and modulus are correlated primarily with the ratio of the number of network-modifiers to network-forming cations, but with substantial effects associated with the identity of network modifying cations. This general correlation likely arises from the effect of network-modifying cations in restricting the flexibility of the polymerized Si-O-Si(Al) bond angles within the amorphous structures. Prospectively, this correlation can be deployed as a guide for determining the likely magnitude of anomalous elastic behavior within compositionally variable silicate glasses.

ACKNOWLEDGMENTS

The glass sample used in this study was kindly provided by Dr. A. Chumakov. This work was supported by the U.S. National Science Foundation (Grants EAR-0074285 and EAR-2017294). We are grateful to the late John Balogh for maintaining the spectroscopic systems at the University of Hawaii, where these measurements were conducted, and to three anonymous reviewers for constructive comments.

Author Contributions

Anwar Hushur: Formal analysis (lead); Investigation (lead); Writing-original draft (equal). **Murli Manghnani:** Formal Analysis (equal); Conceptualization (lead); Investigation (equal); Resources (lead); Funding Acquisition (equal). **Quentin Williams:** Formal Analysis (equal); Resources (equal); Funding acquisition (equal); Writing-original draft (equal).

REFERENCES

1) A. Polian and M. Grimsditch, Room temperature densification of a-SiO_2 versus pressure, Phys. Rev. B, 47, 13979-13982, 1993. https://doi.org/10.1103/PhysRevB.47.13979

2) C.S. Zha, R.J. Hemley, H.K. Mao, T.S. Duffy and C. Meade, Acoustic velocities and refractive-index of SiO_2 glass to 57.5 GPa by Brillouin scattering, Phys. Rev. B, 50, 13105-13112, 1994. https://doi.org/10.1103/PhysRevB.50.13105

3) K. Suito, M. Miyoshi, T. Sasakura, and H. Fujisawa, in *High-Pressure Research: Application to Earth and Planetary Sciences*, edited by Y. Syono and M. H. Manghnani (TERRAPUB, Tokyo, 1992), pp. 219–225.

4) A. Yokoyama, M. Matsui, Y. Higo, Y. Kono, T. Irifune and K.-I. Funakoshi, Elastic wave velocities of silica glass at high temperature and high pressures, J. Appl. Phys. 107, 123530, 2010. https://doi.org/10.1063/1.3452382

5) J.-A. Xu, Brillouin scattering and ultrasonic studies at high temperature and high pressure, Chem. Geol., 128, 17-24, 1996. https://doi.org/10.1016/0009-2541(95)00160-3

6) S.N. Tkachev, M.H. Manghnani and Q. Williams, In situ Brillouin spectroscopy of a pressure-induced apparent second-order transition in a silicate glass, Phys. Rev. Lett., 95, 057402, 2005. https://doi.org/10.1103/PhysRevLett.95.057402

7) C. Sanchez-Valle and J.D. Bass, Elasticity and pressure-induced structural changes in vitreous $MgSiO_3$-enstatite at high pressures, Earth Planet. Sci. Lett., 295, 523-530, 2010. https://doi.org/10.1016/j.epsl.2010.04.034

8) C. Sonneville, D. De Ligny, A. Mermet, B. Champagnon, C. Martinet, G.H. Henderson, T. Deschamps, J. Margueritat and E. Barthel, In situ Brillouin study of sodium alumino silicate glasses under pressure, J. Chem. Phys. 139, 074501, 2013. https://doi.org/10.1063/1.4818335

9) J. Liu and J.-F. Lin, Abnormal acoustic wave velocities in basaltic and (Fe,Al)-bearing silicate glasses at high pressures, Geophys. Res. Lett, 41, 8832-8839, 2014. https://doi.org/10.1002/2014GL062053

10) T. Sakamaki, Y. Kono, Y. Wang, C. Park, T.Yu, Z. Jing and G. Shen, Contrasting sound velocity and intermediate-range order between polymerized and depolymerized silicate glasses under pressure, Earth Planet. Sci. Lett., 391, 288-295, 2014. https://doi.org/10.1016/j.epsl.2014.02.008

11) A.N. Clark, C.E. Lesher, S.D. Jacobsen and Y. Wang, Anomalous density and elastic properties of basalt at high pressure: Reevaluating of the effect of melt fraction on seismic velocity in the Earth's crust and upper mantle, J. Geophys. Res., 121, 4232-4248, 2016. https://doi.org/10.1002/2016JB012973

12) M.H. Manghnani, Q. Williams, T. Matsui, P.C. Schultz and C.R. Kurkjian, Effects of composition, pressure, and temperature on the elastic properties of SiO_2-TiO_2 glasses: An integrated ultrasonic and Brillouin study, Minerals, 10, 481, 2020. https://doi.org/10.3390/min10050481

13) K. Aoki, T. Ohashi, O. Ikeda and A. Suzuki, Effects of alkali and alkaline-earth cations on the high-pressure sound velocities of aluminosilicate glasses, Phys. Chem. Minerals, 47, 28, 2020. https://doi.org/10.1007/s00269-020-01098-3

14) A.I. Chumakov, G. Monaco, A. Monaco, W.A. Crichton, A. Bosak, R. Ruffer, A. Meyer, F. Kargl, L. Comez, D. Fioretto, H. Giefers, S. Roitsch, G. Wortmann, M.H. Manghnani, A. Hushur, Q. Williams, J. Balogh, K. Parlinski, P. Jochym and P. Piekarz, Equivalence of the boson peak in glasses to the transverse acoustic van Hove singularity in crystals, Phys. Rev. Lett., 106, 225501, 2011. https://doi.org/10.1103/PhysRevLett.106.225501

15) P.A. Bingham, J.M. Parker, T.M. Searle and I. Smith, Local structure and medium range ordering of tetrahedrally coordinated Fe^{3+} ions in alkali-alkaline earth-silica glasses, J. Non-Cryst. Solids, 353, 2479, 2007. https://doi.org/10.1016/j.jnoncrysol.2007.03.017

16) J.E. Shelby, Thermal expansion of mixed alkali-silicate glasses, J. Appl. Phys., 47, 4489-4496, 1976. https://doi.org/10.1063/1.322418

17) R. Knoche, D.B. Dingwell, F.A. Seifert and S.L. Webb, Nonlinear properties of supercooled liquids in the system Na_2O-SiO_2, Chem. Geol., 116, 1-16, 1994. https://doi.org/10.1016/0009-2541(94)90154-6

18) A. Monaco, A.I. Chumakov, G. Monaco, W.A. Crichton, A. Meyer, L. Comez, D. Fioretto, J. Korecki and R. Ruffer, Effect of densification on the density of vibrational states of glasses, Phys. Rev. Lett., 97, 135501, 2006. https://doi.org/10.1103/PhysRevLett.97.135501

19) E.H. Hamilton, and G.W. Cleek, Properties of sodium titanium silicate glasses, J. Nat. Bur. Stand., 61, 89-94, 1958.

20) P. Richet and Y. Bottinga, Heat capacity of liquid silicates: New measurements on $NaAlSi_3O_8$ and $K_2Si_4O_9$, Geochim. Cosmochim. Acta, 44, 1535-1541, 1980. https://doi.org/10.1016/0016-7037(80)90117-9

21) T. Rouxel, H. Ji, T. Hammouda and A. Moreac, Poisson's ratio and the densification of glass under high pressure, Phys. Rev. Lett., 100, 225501, 2008. https://doi.org/10.1103/PhysRevLett.100.225501

22) Z. Wang, T.F. Cooney and S.K. Sharma, In situ structural investigation on iron-containing silicate liquids and glasses, Geochim. Cosmochim. Acta, 59, 1571, 1995. https://doi.org/10.1016/0016-7037(95)00063-6

23) D. Di Genova, J. Vasseur, K.-U. Hess, D.R. Neuville and D.B. Dingwell, Effect of oxygen fugacity on the glass transition, viscosity ad structure of silica- and iron-rich

magmatic melts, J. Non-Cryst. Solids, 470, 78, 2017.
http://dx.doi.org/10.1016/j.jnoncrysol.2017.05.013

24) B. Champagnon, C. Martinet, M. Boudeulle, D. Vouagner, C. Coussa, T. Deschamps and L. Grosvalet, High pressure elastic and plastic deformations of silica: In situ diamond anvil cell experiments, J. Non-Cryst. Solids, 354, 569, 2008.
https://doi.org/10.1016/j.jnoncrysol.2007.07.079

25) T. Sato, N. Funamori and T. Yagi, Helium penetrates into silica glass and reduces its compressibility, Nat. Comm., 2, 345, 2011. https://doi.org/10.1038/ncomms1343

26) G. Shen, Q. Mei, V.B. Prakapenka, P. Lazor, S. Sinogeikin, Y. Meng and C. Park, Effect of helium on structure and compression behavior of SiO_2 glass, Proc. Natl. Acad. Sci., 108, 6004-6007, 2011. https://doi.org/10.1073/pnas.1102361108

27) C. Weigel, A. Polian, M. Kint, B. Ruffle, M. Foret and R. Vacher, Vitreous silica distends in helium gas: Acoustic versus static compressibilities, Phys. Rev. Lett., 109, 245504, 2012. https://doi.org/10.1103/PhysRevLett.109.245504

28) B.Y. Chen, S.D. Mahanti and M. Yussouff, Helium atoms in zeolite cages: Novel Mott-Hubbard and Bose-Hubbard systems. Phys. Rev. Lett., 75, 473-477, 1995.
https://doi.org/10.1103/PhysRevLett.75.473

29) N.L. Ross, and E.P. Meagher, A molecular orbital study of $H_6Si_2O_7$ under simulated compression, Am. Mineral., 69, 1145-1149, 1984.

30) T.J. Sokolowski and M.H. Manghnani, Adiabatic elastic moduli of vitreous calcium aluminates to 3.5 kbar, J. Am. Ceram. Soc., 52, 539-542, 1969.
https://doi.org/10.1111/j.1151-2916.1969.tb09160.x

31) M. Guerette, M.R. Ackerson, J. Thomas, F. Yuan, E.B. Watson, D. Walker and L. Huang, Structure and properties of silica glass densified in cold compression and hot compression, Sci. Reports 5, 15343, 2015. https://doi.org/10.1038/srep15343

32) C. Sonneville, A. Mermet, B. Champagnon, C. Martinet, J. Margueritat, D. de Ligny, T. Deschamps and F. Balima, Progressive transformations of silica glass upon densification, J. Chem. Phys. 137, 124505, 2012. https://doi.org/10.1063/1.4754601

33) K.O. Trachenko, M.T. Dove, M.J. Harris and V. Heine, Dynamics of silica glass: two-level tunnelling states and low-energy floppy modes, J. Phys. Cond. Matter, 12, 8041, 2000. https://doi.org/10.1088/0953-8984/12/37/304

34) M. Wyart, H. Liang, A. Kabla and L. Mahadevan, Elasticity of floppy and stiff random networks, Phys. Rev. Lett., 101, 215501, 2008.
https://doi.org/10.1103/PhysRevLett.101.215501

35) E. DeGiuli, A. Laversanne-Finot, G. During, E. Lerner and M. Wyart, Effects of coordination and pressure on sound attenuation, boson peak and elasticity in amorphous solids, Soft Matter, 10, 5628, 2014. https://doi.org/10.1039/c4sm00561a

36) Y. Kikuchi, H. Sudo and N. Kuzuu, Thermal expansion of vitreous silica: Correspondence between dilatation curve and phase transitions in crystalline silica, J. Appl. Phys., 82, 4121, 1997. https://doi.org/10.1063/1.366279

37) J.E. Shelby, Formation and properties of calcium aluminosilicate glasses, J. Am. Ceram. Soc., 68, 155, 1985. https://doi.org/10.1111/j.1151-2916.1985.tb09656.x

38) A. Goel, D.U. Tulyaganov, S. Agathopoulos, M.J. Ribeiro and J.M.F. Ferreira, Synthesis and characterization of $MgSiO_3$-containing glass-ceramics, Ceram. Internat., 33, 1481, 2007. https://doi.org/10.1016/j.ceramint.2006.05.012

39) G. Scannell, A. Koike and L. Huang, Structure and thermos-mechanical response of TiO_2-SiO_2 glasses to temperature, J. Non-Cryst. Solids, 447, 238, 2016. http://dx.doi.org/10.1016/j.jnoncrysol.2016.06.018

40) P.S. Salmon et al., Pressure induced structural transformations in amorphous $MgSiO_3$ and $CaSiO_3$, J. Non-Cryst. Solids, X 3, 100024, 2019. https://doi.org/10.1016/j.nocx.2019.100024